Geochemical controls on the enrichment of fluoride in the mine water of the Shendong mining area, China

Zheng Zhang [a,b], Guoqing Li [a,b,*], Xianbo Su [b,**], Xinguo Zhuang [b], Lei Wang [b], Haijiao Fu [b], Lin Li [b]

[a] State Key Laboratory of Water Resource Protection and Utilization in Coal Mining, Beijing, 102200, China
[b] School of Earth Resources, China University of Geosciences, Wuhan, 430074, China

ARTICLE INFO

ABSTRACT

Underground coal mining produces large amounts of mine water annually in the Shendong mining area of China. Due to the severe scarcity of water resources, mine water is extensively used for productive, domestic, and ecological demands. However, mine water exhibits high fluoride levels. For water-use security, reduction of fluoride exposure and environmental protection, knowledge of sources and geochemical controls of fluoride enrichment in mine water is required. The results showed that F^- concentrations of mine waters vary from 0.05 to 11.65 mg/L, with a mean value of 1.96 mg/L, and 51% of the mine waters contain F^- concentrations exceeding the Chinese drinking water standard (1 mg/L). The overall mine water quality is influenced by cation exchange, mineral dissolution, pyrite oxidation, silicate weathering and so on. The high-fluoride mine waters are all associated with Na–type, with a remarkable cation composition feature of higher Na^+ and lower Ca^{2+} and Mg^{2+} concentrations. Overall, the high-fluoride mine waters are well-matched with the water environment with higher pH, TDS, and EC levels. PCA reveals that the geochemical controls on the enrichment of F^- in mine waters include dissolution of fluoride-bearing minerals and F^--OH^- ion exchange; the former process is mainly caused by the decrease in Ca^{2+} concentrations resulting from Na^+-Ca^{2+} cation exchange and mineral precipitation, and the latter process benefits from a highly alkaline water environment, facilitating the substitution of OH^- in the mine water for F^- within or absorbed on the minerals. Evaporation also controls F^- enrichment in local areas.

1. Introduction

Fluorine (F) is ubiquitous in organisms and the environment (air, soil, and water) in the form of various compounds, which are dominated by fluoride (Merian et al., 2004; Singh et al., 2018). Fluoride is indispensable for the human body, but the acceptable intake is within a very narrow range (Ayoob and Gupta, 2006; WHO, 2017; Adeyeye et al., 2021). Long-term excessive ingestion of fluorine leads to skeletal or dental fluorosis and some other detrimental effects, including kidney damage, thyroxine changes, and physiological disorders (Reddy et al., 2010; Salifu et al., 2012; Fallahzadeh et al., 2018). Groundwater is the major source of fluoride exposure in humans (Jha et al., 2011; Rashid et al., 2018; He et al., 2020), and thus intake of high-fluoride groundwater is the most significant way to cause fluorosis (Chen et al., 2020a). Fluorosis resulting from drinking high-fluoride groundwater occurs in many parts of the world and has raised global alarm and anguish (Wen et al., 2013; Jadhav et al., 2015; Rashid et al., 2020).

Underground coal mining worldwide commonly brings about the output of large amounts of mine water (Belmer and Wright, 2020; Dong et al., 2021), which are predominantly derived from groundwater. Mine water often contains a variety of contaminants (Cravotta, 2008; Feng et al., 2014; Fleming et al., 2021), such as excessive sulphate, fluoride, and heavy metals, affecting the potential uses of water supplies in coal mining areas, as well as causing environmental dangers (Wolkersdorfer and Bowell, 2005; Arefieva et al., 2019; Pyankov et al., 2021). As the largest coal base in China (Xu et al., 2021) and the only modern mining area with annual 200-million-ton coal production in the world (Gu et al., 2014), the Shendong mining area produces up to approximately 106 million tons of mine water annually due to the large-scale underground coal mining. The climate in the Shendong mining area is arid with little rainfall, and the natural ecological conditions are very fragile with a severe scarcity of water resources (Guo et al., 2020; Song et al., 2020).

The mine water guarantees the water supply for production, living and ecology of the Shendong mining area, nearby power plants, and chemical industry of coal-to-liquid (Gu et al., 2014); in addition, some mine water after simple purification treatment is discharged into rivers or directly on the land surface (Song et al., 2020). However, the concentration of fluoride in the mine water of several coal mines of the Shendong mining area was found to exceed the Chinese drinking water standard (1 mg/L) (Guo et al., 2017), which doubtlessly brings potential crises for the water supply and the ecological environment (such as polluting soil and shallow groundwater) of the mining area.

Fluorine mainly occurs as monovalent fluoride (F^-) in natural waters (WHO et al., 2006). The fluoride concentrations in groundwater are generally lower than 1 mg/L but can be much higher when groundwater is under the appropriate mineralogical and geochemical conditions (Rafique et al., 2015). Fluoride concentrations are mostly governed by water-rock interactions because fluoride primarily originates from the various minerals in rocks (Chae et al., 2007; Reddy et al., 2010; Edmunds and Smedley, 2013). Common fluorine-bearing minerals such as fluorite (CaF_2), topaz ($Al_2(F,OH)SiO_4$), sellaite (MgF_2), cryolite (Na_3AlF_6), fluorapatite ($Ca_5(PO_4)_3F$), amphiboles, biotite, and micas constitute potential sources of fluoride in groundwater (Chae et al., 2007; Brindha and Elango, 2011; Singh et al., 2012; Rafique et al., 2015; Luo et al., 2018). Fluorite (CaF_2) is considered a predominant mineral that controls fluoride concentrations in groundwater in many areas (Salifu et al., 2012; Pettenati et al., 2013), especially in granitic terrains (Shah and Danishwar, 2003; Reddy et al., 2010; Subba Rao et al., 2016). Clay minerals such as smectites, illite, and chlorite can also contribute to fluoride enrichment in groundwater by acting as excellent anion exchange media (Weinstein and Davison, 2004; Brunt et al., 2004; Rafique et al., 2009). Studies have shown that a highly alkaline environment favours the enrichment of fluoride (Rafique et al., 2009; Lü et al., 2016; Rashid et al., 2018). The occurrence of high-fluoride groundwater can also result from evaporation, which may trigger the precipitation of $CaCO_3$ and result in a reduction of Ca^{2+} concentration of the groundwater and consequently facilitate the dissolution of CaF_2 (Rafique et al., 2015; Dehbandi et al., 2017; Li et al., 2018). In addition, anthropogenic sources/industrial activities such as the burning of high-fluoride coal, application of phosphatic fertilizers, use of clays in ceramic industries, and processing of phosphatic raw materials can also lead to excessive amounts of fluoride in groundwater (Brunt et al., 2004; Chen et al., 2010; Salifu et al., 2012; Sahu et al., 2021).

In this study, 51 mine water samples were collected from the underground coal mines of the Shendong mining area and their geochemical data were analysed using Schoeller and Piper diagrams, correlation analysis, and principal component analysis (PCA). The purpose of this study is to investigate the geochemistry of high-fluoride mine water in the Shendong mining area and identify the geochemical processes that control fluoride enrichment in mine water. The results of this study can raise awareness of the mine water quality of the Shendong mining area and help the local environmental protection agency (EPA) and industrial sector make more appropriate plans for the utilization, treatment, and discharge of mine water and coal mining schemes of this mining area.
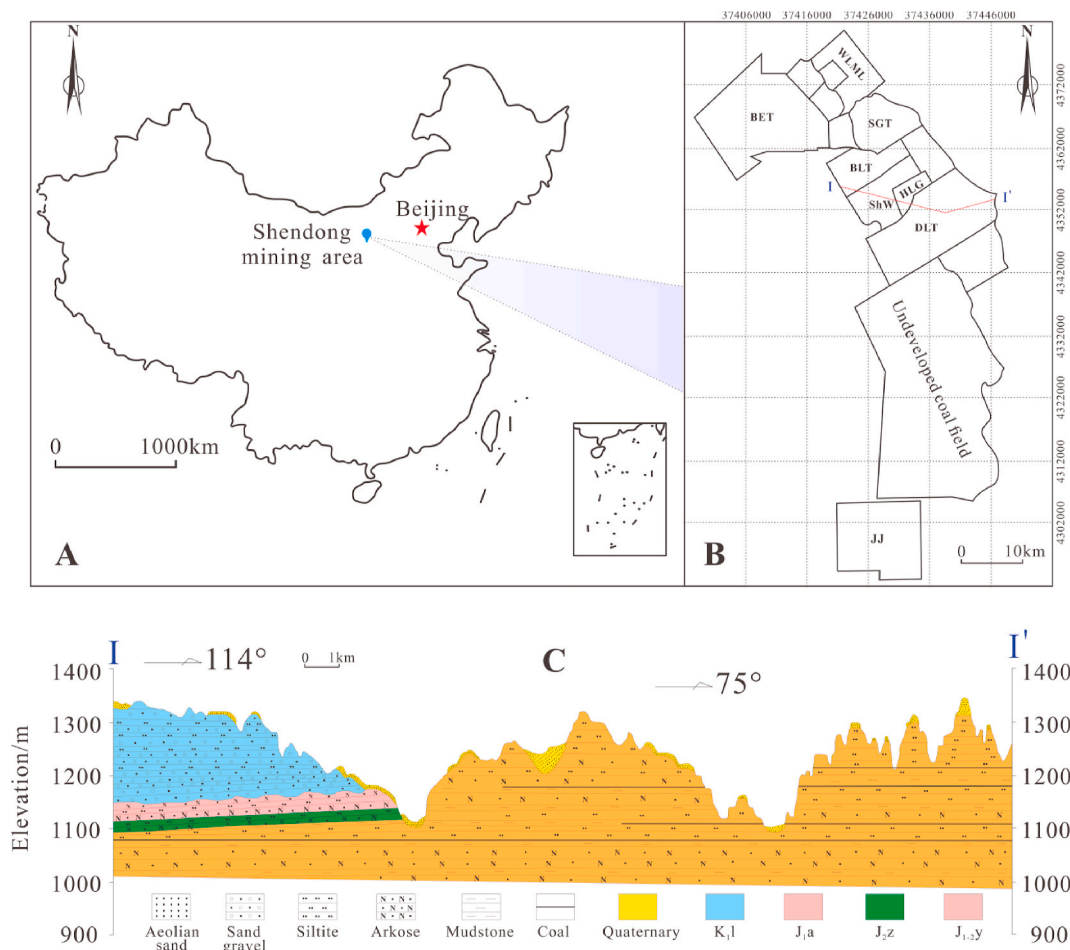
Fig. 1. (A) The location of Shendong mining area in China; (B) The divisions of coal mines of Shendong mining area and the location of coal mines that were sampled; (C) Geological cross-section map of I-I′ (modified from Fu et al., 2018) in the Fig. 1(B).

2. Study area

The Shendong mining area (Fig. 1), covering approximately 3500 km^2, is located at the border of Shaanxi, Inner Mongolia and Shanxi provinces of China. This mining area is characterized by a sparse population and advanced coal mining technology (Guo et al., 2020). It lies at the southeast edge of the Maowusu Desert, with an average elevation of approximately 1200 m. The surface of the mining area is covered by flowing and semifixed sand, with a maximum thickness of up to 20–50 m. The mining area is situated in the arid inland region of Northwest China and has a typical semiarid and semidesert plateau continental climate; the vegetation is scarce, and the ecological environment is very vulnerable (Wang et al., 2008). The annual average temperature is 11.2 °C, and this dry area receives little rain with an average annual precipitation of 320–440 mm; however, the average annual evaporation reaches 2297.4–2838.7 mm, which is 6–7 times the rainfall (Li et al., 2013). Therefore, this region is poor in water resources, and the supply of water for living and production activities in the mining area is very tight. The surface water system in this region is undeveloped, and the main river is the Ulan Mulun River, which flows through the whole mining area. The terrain is cut strongly in this region, which is crisscrossed by ravines and valleys. With respect to structure, the Shendong mining area is located at the slope belt of northern Shaanxi, which is a secondary structural unit of the Ordos Basin. The overall structure of the mining area is a monocline, dipping towards the SW with a dip angle of 1°–6°. Faults are rare in the mining areas, and the structure is simple.

The strata in the Shendong mining area mainly include the Yanchang Formation (T$_{3y}$) of the Upper Triassic, Fuxian Formation (J$_{1f}$) of the Lower Jurassic, Yanan Formation (J$_{1-2y}$) of the Middle and Lower Jurassic, Zhiluo Formation (J$_{2z}$) and Anding Formation (J$_{2a}$) of the Middle Jurassic, and Cenozoic (Kz) from bottom to top. The Luohe Formation (K$_1$l) of the Lower Cretaceous appears in some areas of the study area (Fig. 1C). The main coal seams occur in J$_{1-2y}$, containing five coal groups numbered 1$^\#$–5$^\#$. The coal seams were mainly deposited in lacustrine delta and fluvial sedimentary environments (Wu, 2001). The burial depth of the coal seams varies from 60 to 400 m, with most being approximately 100 m.

Groundwater in this area is relatively scanty, and the total amount is relatively deficient. The groundwater in this area mainly occurs in porous phreatic aquifers of Quaternary and Mesozoic pore-fissure aquifers of clasolite. There are two aquifers that are relatively rich in groundwater in this area, and they are porous phreatic aquifers of the Salawusu Formation (Q$_{3s}$) in the upper Pleistocene of the Quaternary and pore-fissure confined aquifers of the Yanan Formation (J$_{1-2y}$) in the Middle and Lower Jurassic. These two aquifers are also the main water-supplying aquifers for coal mine water in the Shendong mining area.

The Q$_{3s}$ porous phreatic aquifer is mainly distributed in the regions of Daliuta, Shigetai and south Ningtiao. The thickness of this aquifer generally ranges from 10 to 30 m; the lithology is mainly composed of silty-fine and medium-coarse sandstones, with a gravel layer occurring at the bottom of this formation in local areas; overall, the structure of this formation is loose, and precipitation easily infiltrates. The burial depth of the groundwater level of this aquifer generally varies from 0 to 30 m, and the unit water inflow of the borehole ranges from 0.1 to 2.11 L/(s·m). Overall, the water abundance of this aquifer is medium, with strong water in local areas.

The J$_{1-2y}$ pore-fissure aquifer is mainly composed of medium-coarse sandstones, and the fractures are poorly developed overall. The unit water inflow of the borehole of this aquifer varies from 0.00001 to 0.0011 L/(s·m), indicating an overall extremely weak water yield property. However, in some regions, burnt rocks occur in this formation due to the spontaneous combustion of the coal seam, leading to well-developed holes and fractures. The water abundance in holes and fractures of burnt rocks is strong to extremely strong.

3. Materials and methods

3.1. Sampling and sample test

In this study, a total of 51 mine water samples were collected from eight coal mines including Shigetai (SGT), Halagou (HLG), Wulanmulun (WLML), Buertai (BET), Bulianta (BLT), Daliuta (DLT), Shangwan (ShW), and Jingjie (JJ), which cover the main production mines of the Shendong mining area (Fig. 1), during Nov.–Dec. 2019 and Jul.–Aug. 2020. Among the collected mine water samples, there were six samples from SGT, labeled SGT-1–SGT-6; nine from HLG, labeled HLG-1–HLG-9; ten from WLML, labeled WLML-1–WLML-10; three from BET, labeled BET-1–BET-3; five from BLT, labeled BLT-1–BLT-5; ten from DLT, labeled DLT-1–DLT-10; six from ShW, labeled ShW-1–ShW-5; and three from JJ, labeled JJ-1–JJ-3 (Table S1). Samples were obtained from water exploration holes, discharge points of goaf water, and water inlet of the reservoir at underground coal mines.

At each water sampling site of underground coal mines, field measurements, including pH and electrical conductivity (EC), were measured during sample collection using portable meters from Extech Instruments. Before sample collection, the high-density polyethylene (HDPE) bottles were flushed using the target water sample more than three times. In addition, to minimize headspace air, the HDPE bottles were filled to overflow and then capped. Major ion analysis was performed at the State Key Laboratory of Environmental Geochemistry, Institute of Geochemistry Chinese Academy of Sciences within one week after sampling.

Due to suspended particles and insoluble matters containing in the collected water samples, these things may damage and block the pipeline, pump or chromatographic column of the instrument such as Chromatograph. Therefore, each collected water sample was filtered first using a Millipore filter with a 0.45 μm in pore diameter in the laboratory for the security measure of the sophisticated instrument (Gao et al., 2013; Li et al., 2018; Rashid et al., 2021). After that, the filtered sample was divided into two subsamples. One subsample used for major cation analysis was acidified to pH < 2 by adding a few drops of ultra-pure HNO$_3$. The other subsample was left un-acidified for analyses of major anions. The concentration of HCO$_3^-$ was obtained through acid titration. The concentrations of Na$^+$, Ca^{2+}, Mg^{2+} and K$^+$ were determined using inductively coupled plasma-atomic emission spectrometry (Vista-MPX). The concentrations of anions such as SO$_4^{2-}$, Cl$^-$, F$^-$ and NO$_3^-$ were analysed by ion chromatography (IS90). The analysed major ions of all the collected mine water samples from different coal mines are presented in Table S1 of the paper. The tested anion-cation balance of the samples was generally in the range of 5%, with an average of 4.32%.

3.2. Principal component analysis

Principal component analysis (PCA) has been widely used for analysing geochemical data (Rashid et al., 2019a, 2019b, 2019b; Schweitzer et al., 2019), and it is a multivariate technique that can reduce many variables into a few comprehensive indicators (principal components) (Abdi and Williams, 2010). The basis of PCA has been clearly explained both mathematically and qualitatively (Bro and Smilde, 2014). In short, a set of variables that may be correlated is re-expressed in a rotated coordinate system in which as much variance as possible can be explained by the first few dimensions (Xue et al., 2011). PCA is beneficial in investigating correlations among variables in the original dataset since it selects the new axes to lie along directions of the highest correlation (Gotelli and Ellison, 2004). In the present study, PCA was conducted using IBM SPSS Statistics 19.0 to investigate correlations between chemical constituents in mine water.

4. Results

4.1. Overall quality of mine water

The analysed concentrations of major ions, and the tested pH and EC of mine waters collected from the Shendong mining area are summarized in Table 1. Mine waters in the Shendong mining area belong to neutral to alkaline water based on the tested pH values, ranging from 7.00 to 9.19, with an average of 7.91. The EC values of mine waters are between 274 and 5800 μS/cm, with an average of 1737 μS/cm. Overall, approximately 67% of mine waters possess EC values lower than 2000 μS/cm, the permissible threshold for irrigation (Reddy et al., 2014; Zhang et al., 2018). Overall, the EC level of mine waters from ShW is higher than that of other coal mines (Table S1). The total dissolved solids (TDS) contents of mine waters range between 150 and 2858 mg/L, averaging 955 mg/L. Using the World Health Organization (WHO) guideline of 1000 mg/L TDS as a threshold for potable water (WHO, 1996), over 70% mine waters in this area are acceptable for drinking.

The main anions in the mine waters are HCO_3^- (102.84–1304.10 mg/L, avg. 530.22 mg/L), SO_4^{2-} (9.87–1242.10 mg/L, avg. 348.26 mg/L), and Cl^- (4.67–1063.40 mg/L, avg. 155.88 mg/L). NO_3^- is absent in many mine waters, but high NO_3^- concentrations occur locally (Table S1). Among the mine waters, 49% have detectable NO_3^- with concentrations varying from 0.02 to 17.16 mg/L, averaging 2.36 mg/L. In most geologic formations, natural nitrate is lacking; therefore, a high NO_3^- concentration (>5 mg/L) commonly indicates contamination by animal wastes, fertilizers, and/or effluents (Currell et al., 2010). Investigations revealed that a few goafs in the Shendong mining area lie under irrigated farmland (Ren et al., 2007), and shallow groundwater is highly susceptible to pollution from irrigation water and then enters the goaf through the fissure zone of the goaf, thus influencing the mine water quality. Given that 90% of mine water samples have a relatively low concentration of NO_3^- (<2 mg/L), the local high NO_3^- concentrations in mine water samples may result from downwards vertical leakage of shallow groundwater. The major cations in mine waters are dominated by Na^+ (10.53–1345.80 mg/L, avg. 401.73 mg/L), followed by Ca^{2+} (2.45–241.53 mg/L, avg. 65.97 mg/L), Mg^{2+} (0.03–64.62 mg/L, avg. 15.11 mg/L), and K^+ (0.63–13.58 mg/L, avg. 5.25 mg/L). The comparisons of the average concentration of major ions of mine waters from each colliery between summer and winter are presented in Fig.S1. Overall, the changes of average concentrations of most ions in mine waters of each colliery are small between summer and winter, with slightly higher in summer, which may be related to relatively stronger evaporation intensity in summer.

In general, groundwater in recharge areas has relatively higher concentrations of Ca^{2+} and Mg^{2+}, but lower Na^+ and Cl^- concentrations, and Na^+ and Cl^- concentrations increase along groundwater flow paths towards the stagnant and discharge areas of groundwater (Van Voast, 2003; Dahm et al., 2014; Zhang et al., 2019). In addition, both Na^+ and Cl^- of water samples in this study present strong positive correlation with TDS contents (R^2 = 0.94, and 0.82 respectively). Therefore, the spatial variation of Na^+ and Cl^- concentrations can be used to judge the rough direction of groundwater flow. As shown in Fig. S2, in the north part of the Shendong mining area, mine waters of coal mines in the southwest (e.g., BET, BLT, and ShW) overall have higher concentrations of Na^+ and Cl^- than that of coal mines in the northeast (e.g., WLML, SGT, and HLG), implying that the groundwater flow direction is probably from NE to SW in the north part of the Shendong mining area and the northwest direction is near to the recharge area. The mine water of JJ coal mine in the south part of the study area has the lowest concentrations of Na^+ and Cl^-, suggesting that the groundwater flow direction is overall from South to the North in the south part of the Shendong mining area and JJ coal mine is near to the recharge area of groundwater. Overall, Na^+ and Cl^- concentrations of mine waters in ShW and BLT coal mines are relatively higher in the whole area, indicating that these two coal mines may be in the catchment area of the groundwater.

4.2. Fluoride concentration of mine water

The fluoride concentrations of mine waters range from 0.05 to 11.65 mg/L, averaging 1.96 mg/L, which is higher than the WHO safe drinking level of 1.5 mg/L. The Chinese standards for drinking water quality (GB 5749–2006), Chinese standard for groundwater quality (≤class III) (GB/T 14848–2017), and Chinese environmental quality standards for surface water (≤class III) (GB 3838–2002) all set the guide value of fluoride concentration as 1.0 mg/L. Based on the above Chinese standards, mine water of the Shendong mining area of China that has a fluoride concentration higher than 1.0 mg/L is defined as high-fluoride mine water in this study; otherwise, it is defined as low-fluoride mine water. The results show that approximately 51% of the samples are high-fluoride mine water, and the remaining 49% are low-fluoride. Coal mines whose average fluoride concentration (AFC) exceeds 1.0 mg/L include BET (3.89–11.65 mg/L), WLML (0.27–3.07 mg/L), BLT (3.27–5.38 mg/L), ShW (0.63–5.20 mg/L), and DLT (0.52–2.48 mg/L) (Fig. 2), among which BET is the highest, with an AFC of 7.37 mg/L. Mine waters

Table 1
The statistical summary of analytical data for mine water of Shendong coal mining area, China.

Parameters	Number of samples	Minimum	Maximum	Mean	Median
pH	51	7.00	9.19	7.91	7.84
EC (μS/cm)	51	274	5800	1737	1520
Na^+ (mg/L)	51	10.53	1345.80	401.73	316.36
K^+ (mg/L)	51	0.63	13.58	5.25	5.17
Ca^{2+} (mg/L)	51	2.45	241.53	65.97	52.62
Mg^{2+} (mg/L)	51	0.03	64.62	15.11	11.12
Cl^- (mg/L)	51	4.67	1063.40	155.88	43.53
SO_4^{2-} (mg/L)	51	9.87	1242.10	348.26	292.69
HCO_3^- (mg/L)	51	102.84	1304.10	530.22	518.85
F^- (mg/L)	51	0.05	11.65	1.96	1.16
TDS (mg/L)	51	150	2858	955	725
Na^+/Cl^- [a]	51	1.95	26.74	9.24	6.24
Na^+/Ca^{2+} [b]	51	0.14	142.15	17.08	4.06

[a] Na^+/Cl^- refers to molar Na^+/Cl^- ratio.
[b] Na^+/Ca^{2+} refers to equivalent ratio.

Fig. 2. Distribution of F^- concentration of mine waters collected from each mine of Shendong mining area.

collected from coal mines of SGT (0.05–0.80 mg/L), HLG (0.18–4.98 mg/L), and JJ (0.15–0.35 mg/L) all have AFCs lower than 1.0 mg/L, and JJ possesses the lowest AFC, with a value of only 0.22 mg/L.

The spatial variation of fluoride concentrations of mine waters have been presented in Fig.S3. In the north part of the Shendong mining area, mine waters of coal mines in the southwest (e.g., BET, BLT, and ShW) overall have higher fluoride concentrations than that of coal mines in the northeast (e.g., WLML, SGT, and HLG), that is, the fluoride concentration of mine waters increases from NE to SW direction. The mine water of JJ coal mine in the south part of the study area has the lowest average fluoride concentration. Compare Fig.S2 and Fig.S3, it can be easily discovered that the fluoride concentration in the mine water is influenced by the flow field of groundwater, implying that the water-rock interactions occurring as groundwater moves along the flow paths has significant controls on the fluoride enrichment in groundwater.

5. Discussions

5.1. Relationships of major ions of mine water

Understanding the relationships between major ions allows for a more accurate assessment of ion sources and hydrochemical processes occurring (Carol et al., 2009; Barzegar et al., 2017; Sahu et al., 2021) in mine waters. If molar Na^+/Cl^- ratios in groundwater are close to 1.0,

halite dissolution constitutes the major source of Na^+ and Cl^- in groundwater (Appelo and Postma, 2005; Yuan et al., 2017). For mine waters in this study, a strong positive correlation exists between Na^+ and Cl^- concentrations with a correlation coefficient up to 0.901; however, all mine waters have molar Na^+/Cl^- ratios much greater than 1.0 (Fig. 3a, Table 1), indicating that Na^+ has other major sources, such as Na^+-Ca^{2+} cation exchange (Currell et al., 2011; Li et al., 2015; Wang et al., 2018) and silicate (e.g., albite) weathering reactions (Guo et al., 2007; Rice et al., 2008; Adimalla and Li, 2018). However, the poor correlation between Na^+ and HCO_3^- concentrations suggests that Na^+ concentrations were probably weakly influenced by silicate weathering (Cheung et al., 2010) (Fig. 3b). The relation of (Na^+-Cl^-) versus $(Ca^{2+}+Mg^{2+})-(HCO_3^-+SO_4^{2-})$ has been widely used to identify ion exchange processes (Barzegar et al., 2017; Luo et al., 2018; Chen et al., 2020b). If cation exchange is a significant controlling process for groundwater compositions, the relation between $(Na^+-Cl^-$, meq/L) and $(Ca^{2+}+Mg^{2+})-(HCO_3^-+SO_4^{2-})$ (meq/L) should be linear with a slope of -1.0. Fig. 3c shows that all the mine waters are distributed around the line (slope of -1.0) and define a straight line (r = 0.991) with a slope of -0.863, indicating that cation exchange reactions were ubiquitous in mine waters. In general, groundwater in recharge areas has relatively higher concentrations of Ca^{2+} and Mg^{2+}, but lower Na^+ concentrations and Na^+ concentrations increase along groundwater flow paths towards the stagnant and discharge areas of groundwater (Van Voast, 2003; Dahm et al., 2014; Zhang et al., 2019). For many basins, the higher Na^+
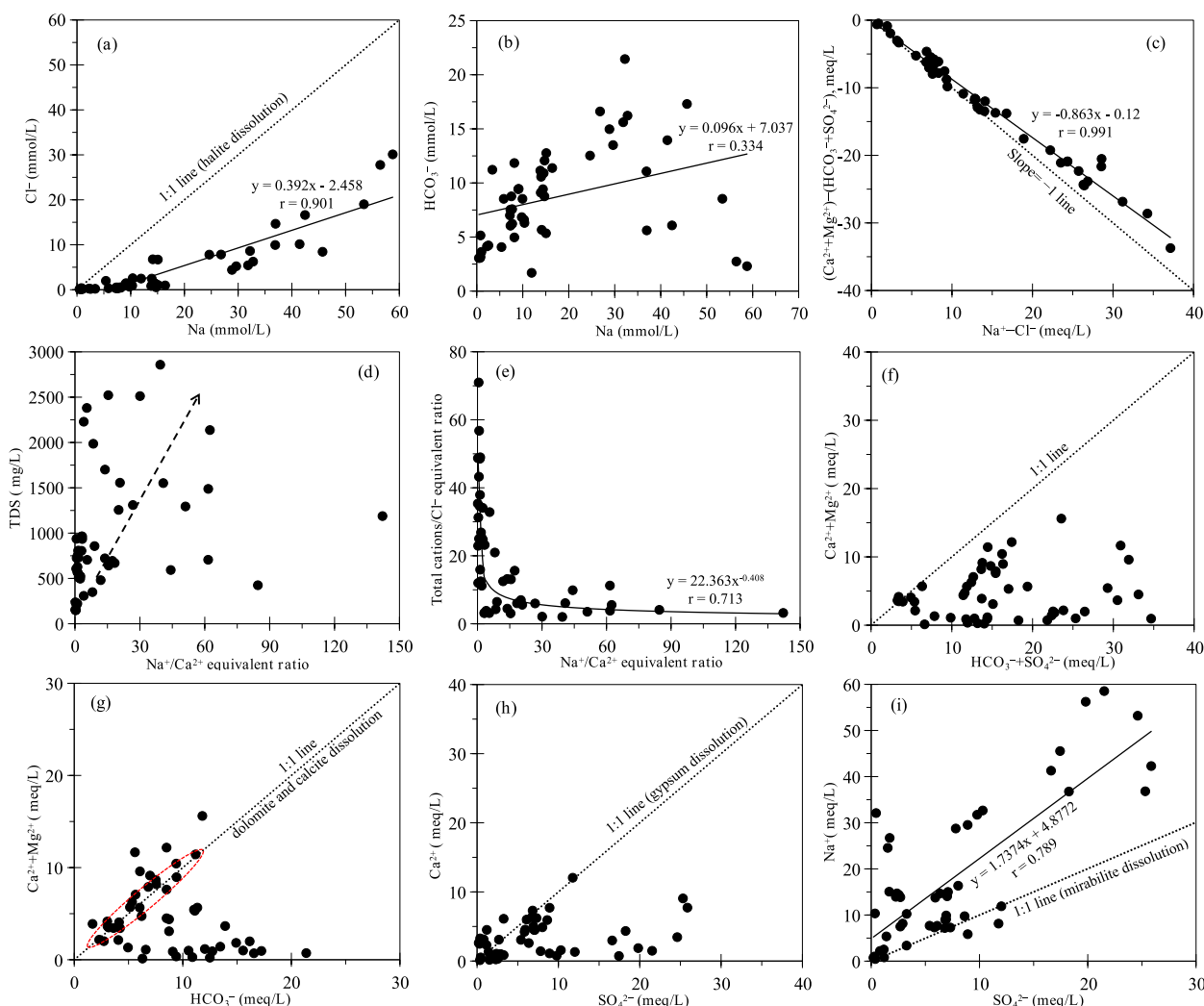
Fig. 3. Ions scatter diagrams for mine waters collected from the Shendong mining area.

concentration in the groundwater of stagnant and discharge areas is related to cation exchange of Ca^{2+} in the groundwater for Na^+ absorbed on the minerals (Guo et al., 2007; Currell et al., 2011). In this study, Na^+/Ca^{2+} equivalent ratios in the mine waters increase with increasing TDS contents except for several outliers (Fig. 3d) but are negatively related to total cation/Cl^- equivalent ratios (r = 0.713) (Fig. 3e); thus, it can be inferred that the increase in Na^+/Ca^{2+} equivalent ratios in mine waters is primarily due to cation exchange of Na^+-Ca^{2+} rather than progressive dissolution of Na-bearing minerals (e.g., albite) (Currell et al., 2011).

If Ca^{2+}, Mg^{2+}, SO_4^{2-} and HCO_3^- in groundwater were derived from a simple mixture of dissolution of dolomite, gypsum, and calcite, then an approximate 1:1 line should hold for the relation between (SO_4^{2-}+HCO_3^-, meq/L) and (Ca^{2+}+Mg^{2+}, meq/L) (Fisher and Mulican, 1997; Wang et al., 2016). However, almost all mine waters in this study fall below the 1:1 line (Fig. 3f), indicating that Ca^{2+}, Mg^{2+}, SO_4^{2-} and HCO_3^- of mine waters are not derived from simple dissolution of dolomite, gypsum, and calcite, and the excess negative charge of HCO_3^- and SO_4^{2-} must be balanced by Na^+, the only other major cation in mine waters. As mentioned above, cation exchange of Na^+-Ca^{2+} was ubiquitous in mine waters, which can also make the data points move away from the 1:1 line of (SO_4^{2-}+HCO_3^-, meq/L) versus (Ca^{2+}+Mg^{2+}, meq/L). Fig. 3g shows that approximately 40% of mine waters fall on or near to the 1:1 line of HCO_3^- (meq/L) versus (Ca^{2+}+Mg^{2+}, meq/L) (inside the dotted line of the ellipse), and the line represents the dissolution of dolomite and calcite (carbonate minerals) by H_2CO_3, and the main reactions are as Eqs. (1)–(3); a few samples are situated above and to the left of the line, possibly indicating excess Ca^{2+} and Mg^{2+} from the dissolution of sulphate or reverse cation exchange of Na^+-Ca^{2+}; however, a large proportion of samples are below and to the right of the line, suggesting excess HCO_3^- that may be derived from other processes, such as silicate weathering (e.g., plagioclase, Equation (4)), and methyl-fermentation process (Equation (5)) in the coal seam (Whiticar, 1999; Flores, 2014), which can generate CO_2 and then form HCO_3^- through Equation (6).

Dissolution of carbonate:

$$CaCO_3 + CO_2 + H_2O \rightarrow Ca^{2+} + 2HCO_3^- \tag{1}$$

$$CaMg(CO_3)_2 + 2CO_2 + 2H_2O \rightarrow Ca^{2+} + Mg^{2+} + 2HCO_3^- \tag{2}$$

$$CaMg(CO_3)_2 + CaCO_3 + 3CO_2 + 3H_2O \rightarrow 2Ca^{2+} + Mg^{2+} + 6HCO_3^- \tag{3}$$
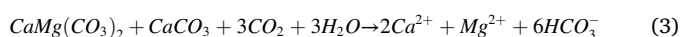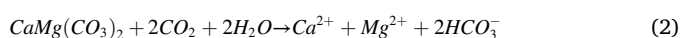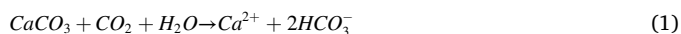
Plagioclase weathering:

$$Na_{0.62}Ca_{0.38}Al_{1.38}Si_{2.62}O_8 + 1.38CO_2 + 4.55H_2O \rightarrow 0.69Al_2Si_2O_5(OH)_4$$
$$+ 0.62Na^+ + 0.38Ca^{2+} + 1.24H_4SiO_4 + 1.38HCO_3^- \tag{4}$$

$$Methyl-fermentation\ process: CH_3COOH \rightarrow CO_2 + CH_4 \tag{5}$$

$$CO_2 + H_2O \rightleftharpoons HCO_3^- + H^+ \tag{6}$$
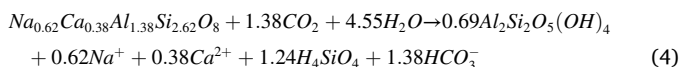
To assess the effect of gypsum dissolution on the compositions of mine waters, the diagram of SO_4^{2-} versus Ca^{2+} is plotted in Fig. 3h, which shows that only approximately 20% of mine waters fall on the 1:1 line reflecting gypsum dissolution. Most mine waters are situated below and to the right of the line, typically interpreted as an excess of SO_4^{2-} derived from other processes (Tarki et al., 2011). The total sulfur content ($S_{t,\ d}$) in the coals of the Shendong mining area is generally 0.2–0.8% with an average of 0.4% and, mainly consists of pyrite sulfur (Qi, 2001; Bai et al., 2002). Coal mining activities make the coal seam and mine water in an oxidizing environment, leading to the oxidation of pyrite in the coal seam and the formation of SO_4^{2-}, and the reaction is equation (7) (Banks et al., 1997). In addition, Fig. 3i shows that SO_4^{2-} has a good positive correlation (r = 0.789) with Na^+, and some mine waters (approximately 17%) fall on the 1:1 line, representing mirabilite dissolution, indicating that mirabilite dissolution may also be one of the

sources of SO_4^{2-}.

$$4FeS_2 + 15O_2 + 14H_2O \rightarrow 4Fe(OH)_3 + 8SO_4^{2-} + 16H^+ \tag{7}$$
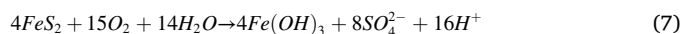
5.2. Geochemistry of high-fluoride mine water

5.2.1. Ionic compositions and hydrochemical types

A Schoeller diagram displaying the major ionic compositions of each mine water is presented in Fig.S4. Compared with low-fluoride mine waters, mine waters with high F^- concentrations have distinctive major ionic compositions, being Na-rich, Cl-rich, Ca-poor, Mg-poor and having relatively higher concentrations of HCO_3^- and SO_4^{2-} (Fig.S4; Table S2). The average concentrations of Na^+ and Cl^- in high-fluoride mine waters are up to 3.99 and 13.29 times those in low-fluoride mine waters, while the average Ca^{2+} and Mg^{2+} concentrations are only 0.45 and 0.32 times those in low-fluoride mine waters, respectively (Table S2).

A number of studies have shown that the hydrochemical types of groundwater have an important effect on the concentrations of F^- in groundwater (Chae et al., 2007; Rafique et al., 2015; Li et al., 2019). The major ionic compositions of sampled mine waters along with F^- concentrations were plotted on the Piper diagram, as shown in Fig. 4A, which can separate the low-fluoride mine waters from the high-fluoride mine waters. The mine waters were classified into four hydrochemical types (Chae et al., 2007): Ca-(SO₄)-Cl, Ca-HCO₃, Na-(SO₄)-Cl, and Na-HCO₃ (Fig. 4A). The high-fluoride mine waters were Na-(SO₄)-Cl or Na-HCO₃ type, with Na-HCO₃ type accounting for a relatively larger proportion. The low-fluoride mine waters were distributed in all four hydrochemical types but with different proportions, 40% of Ca-HCO₃ type, 28% of Na-HCO₃ type, 16% of Ca-(SO₄)-Cl type, and 16% of Na-(SO₄)-Cl type. That is, all the high-fluoride mine waters are of Na-type; 56% low-fluoride mine waters are of Ca-type, and the remaining 44% are Na-type. The F^- concentration of each hydrochemical type is different (Fig. 4B). Na-HCO₃ type mine waters exhibit the highest average F^- concentration with a value of 2.89 mg/L, while mine waters with the Ca-(SO₄)-Cl type show the lowest average F^- concentration with a value of 0.25 mg/L. In addition, the average F^- concentrations of Na-(SO₄)-Cl and Ca-HCO₃ type mine waters are 2.15 and 0.35 mg/L, respectively.

5.2.2. pH, TDS, and EC

Fluoride in groundwater easily dissolves, migrates and accumulates in alkaline environments and is rarely detected in groundwater with acidic environments (pH < 7.0) (Wang et al., 2001). A previous study (Ren et al., 1996) showed that the existence of fluorine in groundwater with an alkaline environment has more than ten forms dominated by F^-, MgF^+, and CaF^+, among which F^- commonly accounts for 79–96%, MgF^+ for 3.1–19.2%, and CaF^+ for 0.3–3.0% of total fluoride concentrations; with the increases of alkaline, the activity of F^- heightens, while the activities of MgF^+ and CaF^+ decrease. On the other hand, within an alkaline environment, groundwater is relatively rich in OH^-; F^- has the same potential and similar ionic radius as OH^-, so the OH^- in groundwater easily replaces the exchangeable F^- ions of fluoride-bearing minerals (such as clay minerals and biotite), and then F^- ions are released to the groundwater, increasing the F^- concentration in groundwater (Wen et al., 2013; Li et al., 2015; Lü et al., 2016). In this study, high-fluoride mine waters overall have a relatively higher average pH value (8.08), which is higher than the average pH level (7.91) of all mine waters, while the pH of low-fluoride mine waters is slightly lower, with an average value of 7.73 (Table S2). Fig. 5a shows that a relatively good positive correlation (r = 0.502) exists between F^- concentrations and the pH of mine waters, conforming to the rule that the stronger the alkalinity is, the higher the F^- concentrations.

The F^- concentrations of groundwater are commonly relevant to the TDS contents (Rafique et al., 2009; Chen et al., 2020a) because the enrichment of F^- is generally related to some hydrogeochemical processes, such as water-rock interactions and evaporation. These processes
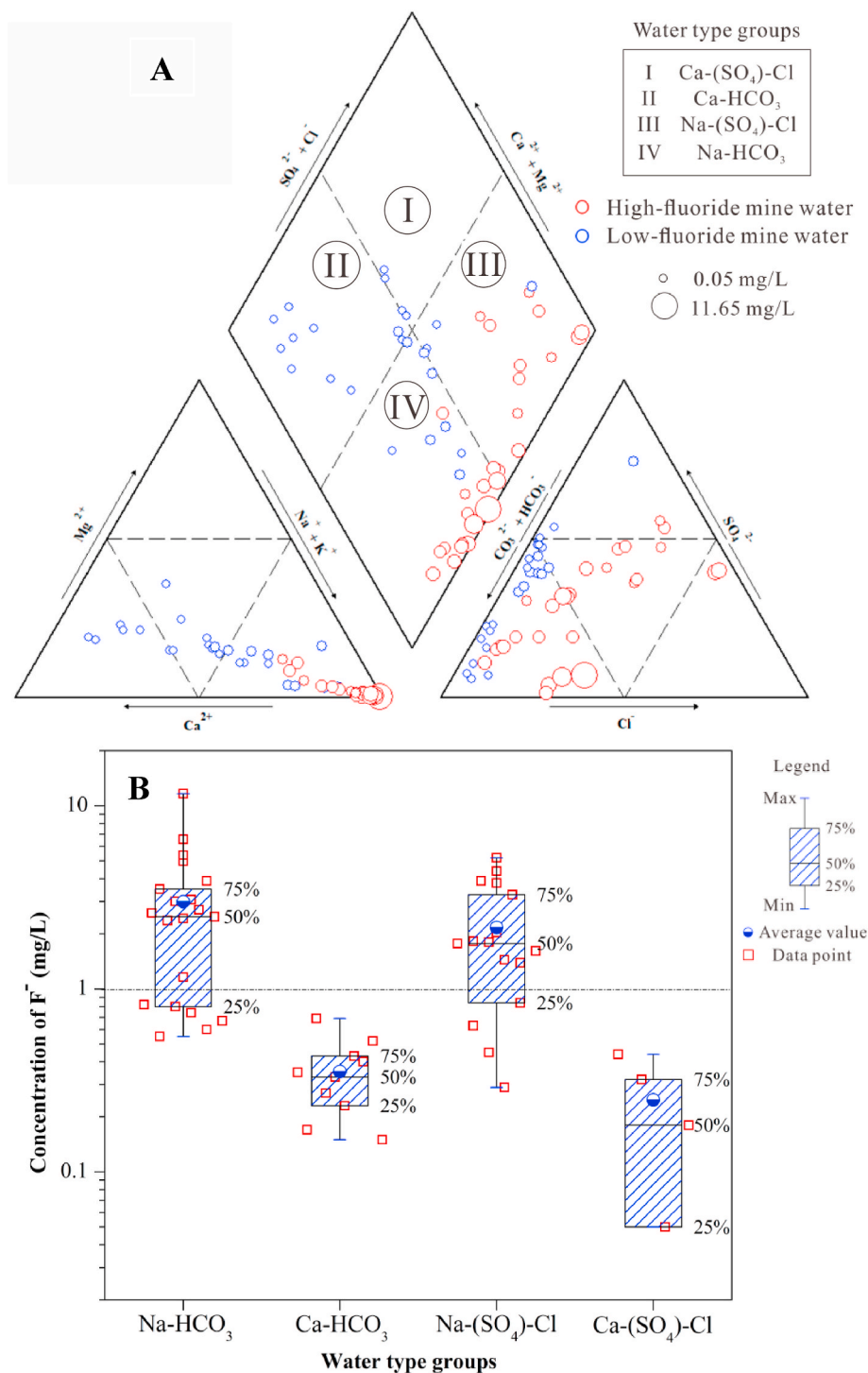
Fig. 4. Piper diagram of major ionic compositions of mine waters of Shendong mining area (A). Box plots show the F^- concentration of mine waters in relation to the hydrochemical types (B).

can change the chemical compositions of the groundwater and then influence the TDS contents. In this study, the average TDS content of high-fluoride mine waters is 1351 mg/L, which is 2.49 times that of low-fluoride mine waters (543 mg/L) (Table S2). Fig. 5b shows that the TDS contents have a relatively good positive correlation (r = 0.529) with F^- concentrations, suggesting that some hydrogeochemical processes control the F^- concentrations in mine waters. Due to a strong positive correlation (r = 0.908) between EC and TDS contents, EC also presents a positive correlation with F^- concentrations (Fig. 5c), possibly implying that higher EC is beneficial to the migration and accumulation of F^- in

groundwater.

5.3. Geochemical processes controlling the fluoride concentrations

To elucidate the geochemical processes controlling the fluoride concentrations in mine waters, PCA was carried out on the F^-, pH, TDS and major ion components of mine waters using the Kaiser-Meyer-Olkin (KMO) and spherical Bartlett tests, and varimax rotation was adopted in the PCA of this work. The results of PCA are shown in Table 2. Two principal components (PCs) were extracted from the nine variables. PC1
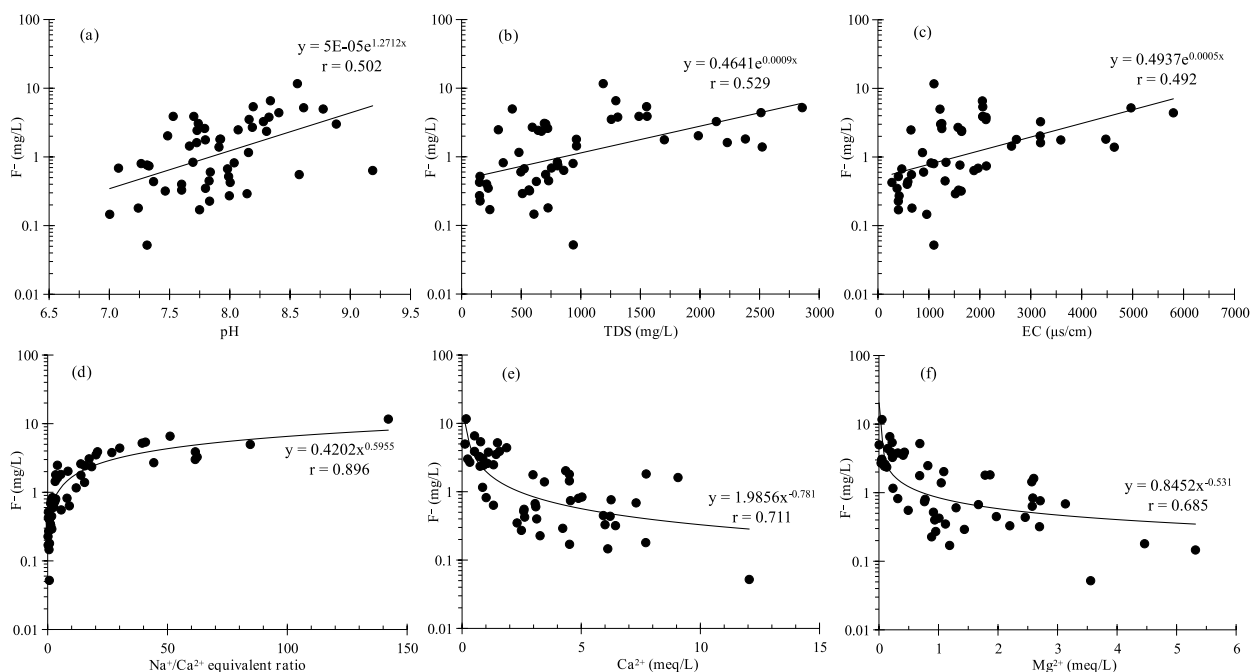
Fig. 5. F^- concentrations versus pH (a), TDS (b), EC values (c), Na^+/Ca^{2+} equivalent ratio (d), Ca^{2+} concentrations (e), and Mg^{2+} concentrations (f) of mine water samples.

Table 2

The loading matrix of varimax rotation factor of chemical compositions of sampled mine waters.

Variable	PC1	PC2
TDS	**0.975**	0.053
Cl^-	**0.938**	0.192
Na^+	**0.930**	0.245
SO_4^{2-}	**0.928**	−0.252
Ca^{2+}	0.121	**−0.933**
Mg^{2+}	−0.026	**−0.868**
pH	0.165	**0.831**
F^-	0.337	**0.663**
HCO_3^-	0.080	0.078
Eigenvalue	3.722	2.923
Contribution rate (%)	41.35	32.48
Cumulative contribution rate (%)	41.35	73.83

The bold represents the variable has considerable impats on the corresponding principal component.

and PC2 described 73.83% of the database variability with 41.35% for PC1 and 32.48% for PC2. Thus, most of the hydrochemical variable information contained in the mine waters can be well explained by the two PCs.

PC1 reveals considerably positive factor loadings for TDS, Cl^-, Na^+, and SO_4^{2-}. PC1 is mostly associated with the dissolution of minerals and cation exchange reactions that occur when groundwater flows from the recharge area to the runoff area and then to the discharge area. Generally, as groundwater moves from the recharge area to the discharge area, Na^+, Cl^-, and TDS concentrations increase due to groundwater-mineral reactions (Van Voast, 2003; Dahm et al., 2014; Zhang et al., 2019). As discussed in Section 4.1, the Cl^- in mine waters of this study mainly comes from halite dissolution. Na^+ is derived from the dissolution of minerals (e.g., halite and mirabilite) and Na^+-Ca^{2+} cation exchange, and the latter is the primary process of Na^+ accumulation in mine waters. SO_4^{2-} in mine waters of this study comes from the dissolution of gypsum and mirabilite and the oxidation of pyrite. Both the dissolution of minerals and cation exchange reactions can lead to an increase in TDS. Therefore, PC1 mostly describes the dissolution of mineral and cation

exchange reactions. Ca^{2+} has a very low positive factor loading in PC1 due to the combined effects of dissolution of minerals (e.g., gypsum) and Na^+-Ca^{2+} cation exchange. The process of gypsum dissolution increases the concentrations of Ca^{2+}, while Na^+-Ca^{2+} cation exchange reduces the concentrations of Ca^{2+} in mine waters.

F^- presents a relatively low positive factor loading (0.337) in PC1, implying that the concentration of F^- in mine waters is associated with the dissolution of mineral and cation exchange reactions. Fig. 5d shows that the Na^+/Ca^{2+} equivalent ratios of mine waters present a strong positive correlation with F^- concentrations, suggesting that Na^+-Ca^{2+} cation exchange has a significant control on the enrichment of F^- in mine water. Na^+-Ca^{2+} cation exchange causes a decrease in Ca^{2+} concentrations and a rise in Na^+ in mine waters, and the decline in Ca^{2+} concentrations facilitates the dissolution of fluorine-bearing minerals, such as fluorite and fluorapatite. The reactions are shown in Eqs. (8) and (9), leading to an increase in F^- concentrations in mine waters. Therefore, all the high-fluoride mine waters are Na-type.

$$CaF_2 \rightleftharpoons Ca^{2+} + 2F^- \tag{8}$$

$$Ca_5(PO_4)_3F \rightleftharpoons 5Ca^{2+} + F^- + 3PO_4^{3-} \tag{9}$$
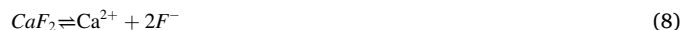
PC2 exhibits considerably negative factor loadings for Ca^{2+} and Mg^{2+} and highly positive factor loadings for F^- and pH. PC2 is possibly associated with mineral precipitation and F^--OH^- ion exchange, resulting from higher pH. From the correlation coefficient matrix in Table S3, it can be observed that the pH presents a relatively good negative correlation with Ca^{2+} (r = −0.668) and Mg^{2+} (r = −0.564) because a higher pH favours the precipitation of $Ca(OH)_2$ and $Mg(OH)_2$ (Eqs. (10) and (11)), resulting in a decrease in Ca^{2+} and Mg^{2+} concentrations in mine waters and thus promoting the dissolution of fluoride-bearing minerals (Eqs. (8) and (9)). Fig. 5e and f also illustrate that the decrease in Ca^{2+} and Mg^{2+} benefits the increase in F^-. In addition, as discussed in Section 5.2.2, due to having the same potential and similar ionic radius as F^-, the OH^- in groundwater easily replaces exchangeable F^- of fluoride-bearing minerals (such as clay minerals and biotite), and then F^- is released to the groundwater, increasing the F^- concentration in groundwater. The reactions in which OH^- in mine waters replaces F

in biotite and muscovite are shown in Eqs. (12) and (13). Clay minerals, such as kaolin, are able to hold F$^-$ on their surfaces, but at higher pH OH$^-$ can displace F$^-$. In summary, an alkaline mine water environment with a higher pH favours the enrichment of F$^-$.

$$Ca^{2+} + 2OH^- \rightleftharpoons Ca(OH)_2 \qquad (10)$$

$$Mg^{2+} + 2OH^- \rightleftharpoons Mg(OH)_2 \qquad (11)$$

$$Biotite : KMg_3(AlSi_3O_{10})F_2 + 2OH^- \rightarrow KMg_3(AlSi_3O_{10})(OH)_2 + 2F^- \qquad (12)$$

$$Muscovite : KAl_2(AlSi_3O_{10})F_2 + 2OH^- \rightarrow KAl_2(AlSi_3O_{10})(OH)_2 + 2F^- \qquad (13)$$
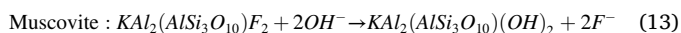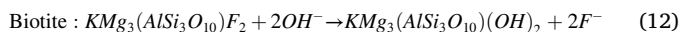
The PCA scores for each mine water marked with the F$^-$ concentration are shown in Fig. 6. As presented in the figure, when mine waters have positive scores on both PC1 and PC2 (first quadrant in Fig. 6), all the mine waters (except one) are characterized by high-fluoride. The average F$^-$ concentration is the highest with a value of 4.74 mg/L because the processes of Na$^+$-Ca^{2+} cation exchange, mineral precipitation and F$^-$-OH$^-$ ion exchange are all relatively intense, lending to the highest F$^-$ concentrations in mine waters. When mine waters have positive scores on PC1 or PC2 (second and fourth quadrants in Fig. 6), it reflects that mineral precipitation and F$^-$-OH$^-$ ion exchange or Na$^+$-Ca^{2+} cation exchange processes are relatively intense, and high-fluoride mine waters also appear with a great probability. Only when mine waters have negative scores on both PC1 and PC2 (third quadrant in Fig. 6), are all the mine waters characterized with low-fluoride, and the average F$^-$ concentration is the lowest with a value of only 0.49 mg/L because Na$^+$-Ca^{2+} cation exchange, mineral precipitation and F$^-$-OH$^-$ ion exchange are all relatively weak. To summarize, the PCA reveals that the geochemical controls on the enrichment of F$^-$ in mine waters of the Shendong mining area include dissolution of fluoride-bearing minerals and F$^-$-OH$^-$ ion exchange. The former is mainly caused by the decrease in Ca^{2+} (and Mg^{2+}) in mine waters resulting from cation exchange or mineral precipitation, and the latter is due to a highly alkaline mine water environment. All these processes that influence the F$^-$ concentrations in mine waters could be attributed to water-rock interactions.

In addition to water-rock interactions, evaporation may also be a factor for the occurrence of high-fluoride mine water in local regions. Data were plotted on Gibbs (1970) diagrams (Fig. 7) to infer the dominant controls on the quality of mine waters. The diagram shows that the vast majority of mine waters are distributed in the region of "rock dominance", suggesting that rock weathering is the most important factor influencing mine water quality. However, several high-fluoride mine water samples fall into the "evaporation dominance" region, revealing that evaporation controls the F$^-$ enrichment of mine waters in local areas. Evaporation may trigger the precipitation of CaCO$_3$ (Dreybrodt and Deininger, 2014; Wallin and Peterman, 2015) and result in a reduction in the Ca^{2+} concentration of the groundwater and consequently facilitate the dissolution of CaF$_2$ (Luo et al., 2018).

6. Conclusions

(1) Mine waters of the Shendong mining area are overall alkalescent with low TDS. The fluoride concentrations range from 0.05 to 11.65 mg/L (avg. 1.96 mg/L), and 51% of the mine waters exceed the Chinese drinking water standard (1 mg/L). Mine water of BET colliery has the highest average fluoride concentration with a value of 7.37 mg/L.
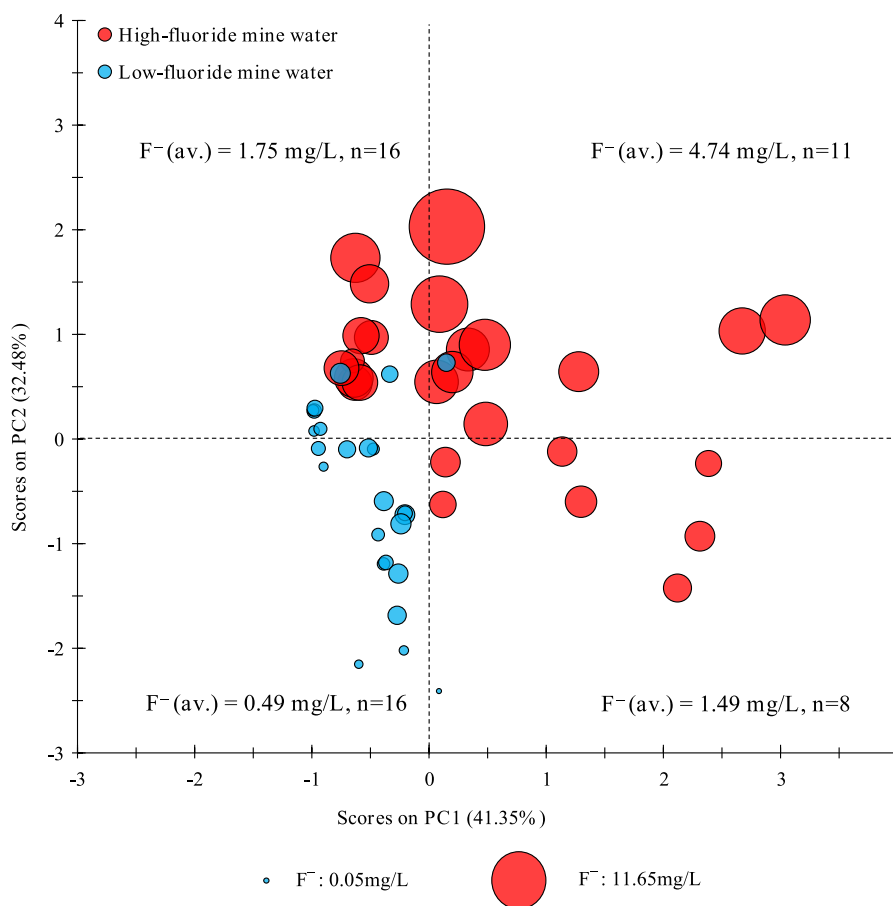
Fig. 6. PCA score plot (PC1 vs. PC2) for high-fluoride and low-fluoride mine waters from Shendong mining area. The size of the circle represents the concentration of F$^-$.
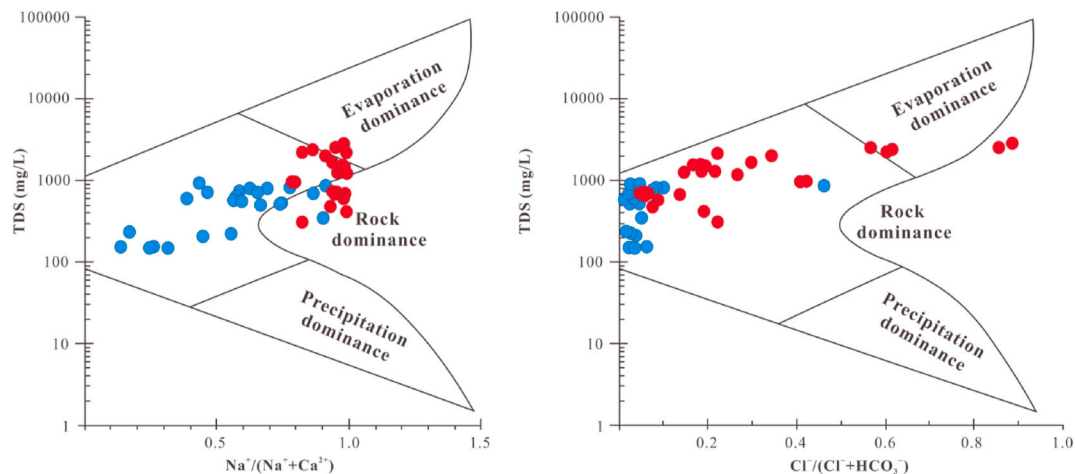
Fig. 7. Gibbs (1970) diagrams (modified by Rashid et al., 2020) showing the mechanism that controls the mine water quality.

(2) Reactions of Na$^+$-Ca^{2+} cation exchange and dissolution of minerals are ubiquitous in mine waters, together with oxidation of pyrite, silicate weathering, and possible methyl-fermentation processes.

(3) High-fluoride mine waters are characterized by Na-rich, Cl-rich, Ca-poor and Mg-poor. All the high-fluoride mine waters are Na-type. Mine waters of the Na-HCO$_3$ type exhibit the highest average F$^-$ concentration with a value of 2.89 mg/L. The fluoride concentrations in mine waters are overall proportional to high pH, high TDS, and high EC levels.

(4) Two PCs were extracted from the chemical parameters, and the contribution rates of PC1 and PC2 are 41.35% and 32.48%, respectively. PCA reveals that the direct geochemical processes that control fluoride enrichment in mine waters include dissolution of fluoride-bearing minerals and F$^-$-OH$^-$ ion exchange; the former process is governed by the consumption of Ca^{2+}, and the latter process benefits from the high pH environment. When the processes of Na$^+$-Ca^{2+} cation exchange, mineral precipitation, and F$^-$-OH$^-$ ion exchange are all relatively strong, the degree of F$^-$ enrichment in mine water is the highest. Evaporation controls the F$^-$ enrichment of mine waters in some areas of the Shendong mining area.

Credit author statement

Zhang Zheng: Conceptualization, Methodology, Investigation, Writing – original draft. Li Guoqing: Writing – review & editing, Investigation, Project administration. Su Xianbo: Validation, Writing – review & editing. Zhuang Xinguo: Writing – review & editing. Wang Lei: Resources, Investigation. Fu Haijiao: Data curation, Formal analysis. Li Lin: Formal analysis.

Declaration of competing interest

The Authors declared that they had no conflicts of interests in their authorship and publication of this Contribution.

Appendix A. Supplementary data

Supplementary data to this article can be found online at https://doi.org/10.1016/j.chemosphere.2021.131388.

References

Abdi, H., Williams, L.J., 2010. Principal component analysis. Wiley Interdiscipl. Rev.: Comput. Stat. 2 (4), 433–459.

Adeyeye, O.A., Xiao, C.L., Zhang, Z.H., Yawe, A.S., Liang, X.J., 2021. Groundwater fluoride chemistry and health risk assessment of multi-aquifers in Jilin Qianan, Northeastern China. Ecotoxicol. Environ. Saf. 211, 111926.

Adimalla, N., Li, P.Y., 2018. Occurrence, health risks, and geochemical mechanisms of fluoride and nitrate in groundwater of the rock-dominant semi-arid region, Telangana State, India. Hum. Ecol. Risk Assess. 25, 81–103.

Appelo, C.A.J., Postma, D., 2005. Geochemistry, Groundwater and Pollution, second ed. A.A. Balkema Publishers, Brookfield, Leiden.

Arefieva, O., Nazarkina, A.V., Gruschakova, N.V., Skurikhina, J.E., Kolycheva, V.B., 2019. Impact of mine waters on chemical composition of soil in the Partizansk Coal Basin, Russia. Int. Soil Water Conserv. Res. 7, 57–63.

Ayoob, S., Gupta, A.K., 2006. Fluoride in drinking water: a review on the status and stress effects. Crit. Rev. Environ. Sci. Technol. 36, 433–487.

Bai, X.F., Li, W.H., Zhang, S.L., Zhao, Y.X., 2002. Study on properties of Shendong Jurassic 2-# coal. Coal Convers. 25 (3), 85–88 (in Chinese with English abstract).

Banks, D., Younger, P.L., Arnesen, R.-T., Iversen, E.R., Banks, S.B., 1997. Mine-water chemistry: the good, the bad and the ugly. Environ. Geol. 32 (3), 157–174.

Belmer, N., Wright, I.A., 2020. The regulation and impact of eight Australian coal mine waste water discharges on downstream river water quality: a regional comparison of active versus closed mines. Water Environ. J. 34 (3), 350–363.

Brindha, K., Elango, L., 2011. Fluoride in groundwater: causes, implications and mitigation measures. In: Monroy, S.D. (Ed.), Fluoride Properties, Applications and Environmental Management, pp. 111–136.

Bro, R., Smilde, A.K., 2014. Principal component analysis. Anal. Methods 6 (9), 2812–2831.

Brunt, R., Vasak, L., Griffion, J., 2004. Fluoride in groundwater: probability of occurrence of excessive concentration on global scale. In: Igrac International Groundwater Resources Assessment Centre.

Barzegar, R., Moghaddam, A.A., Tziritis, E., Fakhri, M.S., Soltani, S., 2017. Identification of hydrogeochemical processes and pollution sources of groundwater resources in the Marand plain, northwest of Iran. Environ. Earth Sci. 76 (7), 297.

Carol, E., Kruse, E., Mas-Pla, J., 2009. Hydrochemical and isotopical evidence of ground water salinization processes on the coastal plain of Samborombón Bay, Argentina. J. Hrdrol. 365, 335–345.

Chae, G., Yun, S., Mayer, B., Kim, K., Kim, S., Kwon, J., Kim, K., Koh, Y., 2007. Fluorine geochemistry in bedrock groundwater of South Korea. Sci. Total Environ. 385, 272–283.

Chen, N., Zhang, Z., Feng, C., Zhu, D., Yang, Y., Sugiura, N., 2010. Preparation and characterization of granular ceramic containing dispersed aluminum and iron oxides as adsorbents for fluoride removal from aqueous solution. J. Hazard. Mater. 186, 863–868.

Chen, Q., Hao, D.C., Gao, Z.J., Shi, M.J., Wang, M., Feng, J.G., Deng, Q.H., Xia, L., Zhang, C.R., Yu, R.B., 2020a. The Enrichment Process of Groundwater Fluorine in Sea Water Intrusion Area of Gaomi City. https://doi.org/10.1111/gwat.12990. China. Groundwater.

Chen, Q., Jia, G.P., Wei, J.C., Dong, F.Y., Yang, W.G., Hao, D.C., Jia, Z.W., Ji, Y.H., 2020b. Geochemical process of groundwater fluoride evolution along global coastal

plains: evidence from the comparison in seawater intrusion area and soil salinization area. Chem. Geol. 552, 119779.

Cheung, K., Klassen, P., Mayer, B., Goodarzi, F., Aravena, R., 2010. Major ion and isotope geochemistry of fluids and gases from coalbed methane and shallow groundwater wells in Alberta, Canada. Appl. Geochem. 25, 1307–1329.

Cravotta III, C.A., 2008. Dissolved metals and associated constituents in abandoned coal-mine discharges, Pennsylvania, USA. Part 1: constituent quantities and correlations. Appl. Geochem. 23, 166–102.

Currell, M.J., Cartwright, I., Bradley, D.C., Han, D.M., 2010. Recharge history and controls on groundwater quality in the Yuncheng Basin, north China. J. Hydrol. 385, 216–229.

Currell, M., Cartwright, I., Raveggi, M., Han, D.M., 2011. Controls on elevated fluoride and arsenic concentrations in groundwater from the Yuncheng Basin, China. Appl. Geochem. 26, 540–552.

Dahm, K.G., Guerra, K.L., Munakata-Marr, J., Drewes, J.E., 2014. Trends in water quality variability for coalbed methane produced water. J. Clean. Prod. 84, 840–848.

Dehbandi, R., Moore, F., Keshavarzi, B., Abbasnejad, A., 2017. Fluoride hydrogeochemistry and bioavailability in groundwater and soil of an endemic fluorosis belt, central Iran. Environ. Earth. Sci. 76, 177.

Dong, S.N., Wang, H., Guo, X.M., Zhou, Z.F., 2021. Characteristics of water hazards in China's coal mines: a review. Mine Water Environ. 40 (2), 325–333. https://doi.org/10.1007/s10230-021-00770-6.

Dreybrodt, W., Deininger, M., 2014. The impact of evaporation to the isotope composition of DIC in calcite precipitating water films in equilibrium and kinetic fractionation models. Geochem. Cosmochim. Acta 125, 433–439.

Edmunds, W.M., Smedley, P.L., 2013. Fluoride in natural waters. In: Essentials of Medical Geology. Revised Edition, pp. 311–336.

Fallahzadeh, R.A., Miri, M., Taghavi, M., Gholizadeh, A., Anbarani, R., Hoseini-Bandegharaei, A., Ferrante, M., Conti, G.O., 2018. Spatial variation and probabilistic risk assessment of exposure to fluoride in drinking water. Food Chem. Toxicol. 113, 314–321.

Feng, Q.Y., Li, T., Qian, B., Zhou, L., Gao, B., Yuan, T., 2014. Chemical characteristics and utilization of coal mine drainage in China. Mine Water Environ. 33, 276–286.

Fisher, R.S., Mulican, W.F., 1997. Hydrogeochemical evolution of sodium sulphate and sodium-chloride groundwater beneath the Northern Chihuahua desert, Trans-Pecos, Texas, USA. Hydrogeol. J. 10 (4), 455–474.

Fleming, C., Morrison, K., Robba, L., Reynolds, J., Wright, I.A., 2021. 14-month water quality investigation of coal mine discharge on two rivers in NSW, Australia: implications for environmental regulation. Water Air Soil Pollut. 232, 90.

Flores, R.M., 2014. Coal and Coalbed Gas: Fueling the Future. Elsevier Inc. Press, USA.

Fu, C.C., Li, X.Q., Ma, J.F., Gao, M., Liu, L.X., Bai, Z.X., 2018. Groundwater quality assessment and recharge sources of groundwater in coal mining area of Kuye river basin. J. China Hydrogeol. 38 (6), 42–47 (in Chinese with English abstract).

Gao, X.B., Su, C.L., Wang, Y.X., Hu, Q.H., 2013. Mobility of arsenic in aquifer sediments at Datong Basin, northern China: effect of bicarbonate and phosphate. J. Geochem. Explor. 135, 93–103.

Gibbs, R.J., 1970. Mechanisms controlling world water chemistry. Science 170, 1088–1090.

Gotelli, N.J., Ellison, A.M., 2004. A Primer of Ecological Statistics. Sinauer Associates, Sunderland, MA.

Gu, D.Z., 2014. Water resource protection and utilization engineering technology of coal mining in "energy golden triangle" region. Coal Eng. 46 (10), 33–37 (in Chinese with English abstract).

Guo, Q.H., Wang, Y.X., Ma, T., Ma, R., 2007. Geochemical processes controlling the elevated fluoride concentrations in groundwaters of the Taiyuan Basin, Northern China. J. Geochem. Explor. 93, 1–12.

Guo, Y., 2017. The concentrations of F^-, Cl^- and SO_4^{2-} determined by ion chromatography in drinking water of Shendong mining area. China Chem. Trade 9 (10), 111–112 (in Chinese).

Guo, Y.N., Chen, G.Q., Mo, R., Wang, M., Bao, Y.Y., 2020. Benefit evaluation of water and soil conservation measures in Shendong based on particle swarm optimization and the analytic hierarchy process. Water 12 (7), 1955.

He, X.D., Li, P.Y., Ji, Y.J., Wang, Y.H., Su, Z.M., Elumalai, V., 2020. Groundwater arsenic and fluoride and associated arsenicosis and fluorosis in China: occurrence, distribution and management. Expos. Health 12, 355–368.

Jadhav, S.V., Bringas, E., Yadav, G.D., Rathod, V.K., Ortiz, I., Marathe, K.V., 2015. Arsenic and fluoride contaminated groundwaters: a review of current technologies for contaminants removal. J. Environ. Manag. 162, 306–325.

Jha, S.K., Mishra, V.K., Sharma, D.K., Damodaran, T., 2011. Fluoride in the environment and its metabolism in humans. Rev. Environ. Contam. Toxicol. 211, 121–142.

Li, Q., Li, Y.C., Chen, D.Y., Liu, H.P., 2013. The water resource utilization in Shendong mining area. J. Arid Land Resour. Environ. 27 (9), 141–147 (in Chinese with English abstract).

Li, C.C., Gao, X.B., Wang, Y.X., 2015. Hydrogeochemistry of high-fluoride groundwater at Yuncheng Basin, northern China. Sci. Total Environ. 508, 155–165.

Li, D.N., Gao, X.B., Wang, Y.X., Luo, W.T., 2018. Diverse mechanisms drive fluoride enrichment in groundwater in two neighboring sites in northern China. Environ. Pollut. 237, 430–441.

Li, P.Y., He, X.D., Li, Y., Xiang, G., 2019. Occurrence and health implication of fluoride in groundwater of loess aquifer in the Chinese loess plateau: a case study of Tongchuan, northwest China. Expos. Health 11 (2), 95–107.

Lü, J., Qiu, H.Y., Lin, H.B., Yuan, Y., Chen, Z., Zhao, R.R., 2016. Source apportionment of fluorine pollution in regional shallow groundwater at You'xi County southeast China. Chemosphere 158, 50–55.

Luo, W.T., Gao, X.B., Zhang, X., 2018. Geochemical processes controlling the groundwater chemistry and fluoride contamination in the Yuncheng Basin, China-An area with complex hydrogeochemical conditions. PloS One 13 (7), e0199082.

Merian, E., Anke, M., Ihnat, M., Stoeppler, M., 2004. Elements and Their Compounds in the Environment: Occurrence, Analysis and Biological Relevance, vol. 2. Wiley-VCH, Weinheim.

Pettenati, M., Perrin, J., Pauwels, H., Ahmed, S., 2013. Simulating fluoride evolution in groundwater using a reactive multicomponent transient transport model: application to a crystalline aquifer of Southern India. Appl. Geochem. 29, 102–116.

Pyankov, S.V., Maximovich, N.G., Khayrulina, E.A., Berezina, O.A., Shikhov, A.N., Abdullin, R.K., 2021. Monitoring acid mine Drainage's effects on surface water in the Kizel coal basin with Sentinel-2 Satellite images. Mine Water Environ. 1–16. https://doi.org/10.1007/s10230-021-00761-7.

Qi, W., 2001. Coal structure and coal quality in Shendong mining area. Coal Sci. Technol. 29 (8), 43–45 (in Chinese with English abstract).

Rafique, T., Naseem, S., Usmani, T.H., Bashir, E., Khan, F.A., 2009. Geochemical factors controlling the occurrence of high fluoride groundwater in the Nagar Parkar area, Sindh, Pakistan. J. Hazard. Mater. 171, 424–430.

Rafique, T., Naseem, S., Ozsvath, D., Hussain, R., Bhanger, M.I., Usmani, T.H., 2015. Geochemical controls of high fluoride groundwater in Umarkot sub-district, thar desert, Pakistan. Sci. Total Environ. 530–531, 271–278.

Rashid, A., Guan, D.X., Farooqi, A., Khan, S., Zahir, S., Jehan, S., Khattak, S.A., Khan, M.S., Khan, R., 2018. Fluoride prevalence in groundwater around a fluorite mining area in the flood plain of the River Swat, Pakistan. Sci. Total Environ. 508, 203–215.

Rashid, A., Khattak, S.A., Ali, L., Zaib, M., Jehan, S., Ayub, M., Ullah, S., 2019a. Geochemical profile and source identification of surface and groundwater pollution of District Chitral, Northern Pakistan. Microchem. J. 145, 1058–1065.

Rashid, A., Khan, S., Ayub, M., Sardar, T., Jehan, S., Zahir, S., Khan, M.S., Muhammad, J., Khan, R., Ali, A., Ullah, H., 2019b. Mapping human health risk from exposure to potential toxic metal contamination in groundwater of Lower Dir, Pakistan: application of multivariate and geographical information system. Chemosphere 225, 785–795.

Rashid, A., Farooqi, A., Gao, X.B., Zahir, S., Noor, S., Khattak, J.A., 2020. Geochemical modeling, source apportionment, health risk exposure and control of higher fluoride in groundwater of sub-district Dargai, Pakistan. Chemosphere 243, 125409.

Rashid, A., Ayub, M., Javed, A., Khan, S., Gao, X.B., Li, C.C., Ullah, Z., Sardar, T., Muhammad, J., Nazneen, S., 2021. Potentially harmful metals, and health risk evaluation in groundwater of Mardan, Pakistan: application of geostatistical approach and geographic information system. Geosci. Front. 12, 101128.

Reddy, D.V., Nagabhushanam, P., Sukhija, B.S., Reddy, A.G.S., Smedley, P.L., 2010. Fluoride dynamics in the granitic aquifer of the Wailapally watershed, Nalgonda district, India. Chem. Geol. 269, 278–289.

Reddy, K.J., Whitman, A.J., Kniss, A.R., 2014. Potential beneficial uses of coalbed natural gas (CBNG) water. Environ. Sci. Proc. Imp. 16 (1), 148–158.

Ren, F.R., Zeng, J.H., Liu, W.S., Zhang, C.Y., 1996. Hydrogeochemical environment of high fluorine groundwater and the relation between the speciation of fluorine and the diseased ratio of endemic fluorosis—a case study of the North China Plain. Acta Geosci. Sin. 17 (1), 85–97 (in Chinese with English abstract).

Ren, Y.Y., 2007. Collapse by Excavating Coal Influence on Farmland Productivity in Shendong Coal. Master thesis. Inner Mongolia Agricultural University, Hohhot, China (in Chinese with English abstract).

Rice, C.A., Flores, R.M., Stricker, G.D., Ellis, M.S., 2008. Chemical and stable isotopic evidence for water/rock interaction and biogenic origin of coalbed methane, Fort Union Formation, Powder River Basin, Wyoming and Montana U.S.A. Int. J. Coal Geol. 76, 76–85.

Sahu, S., Gogoi, U., Nayak, N.C., 2021. Groundwater solute chemistry, hydrogeochemical processes and fluoride contamination in phreatic aquifer of Odisha, India. Geosci. Front. 12, 101093.

Salifu, A., Petrusevski, B., Ghebremichael, K., Buamah, R., Amy, G., 2012. Multivariate statistical analysis for fluoride occurrence in groundwater in the Northern region of Ghana. J. Contam. Hydrol. 140–141, 34–44.

Schweitzer, H., Ritter, D., McIntosh, J., Barnhart, E., Cunningham, A.B., Vinson, D., Orem, W., Fields, M.W., 2019. Changes in microbial communities and associated water and gas geochemistry across a sulfate gradient in coal beds: powder River Basin, USA. Geochem. Cosmochim. Acta 245, 495–513.

Shah, M.T., Danishwar, S., 2003. Potential fluoride contamination in the drinking water of Naranji area, northwest frontier province, Pakistan. Environ. Geochem. Health 25, 475–481.

Singh, C.K., Kumari, R., Singh, N., Mallick, J., Mukherjee, S., 2012. Fluoride enrichment in aquifers of the Thar Desert: controlling factors and its geochemical modelling. Hydrol. Process. 27 (17), 2462–2474.

Singh, G., Kumari, B., Sinam, G., Navin Kumar, K., Mallick, S., 2018. Fluoride distribution and contamination in the water, soil and plants continuum and its remedial technologies, an Indian perspective – a review. Environ. Pollut. 239, 95–108.

Song, H.Q., Xu, J.J., Fang, J., Cao, Z.G., Yang, L.Z., Li, T.X., 2020. Potential for mine water disposal in coal seam goaf: investigation of storage coefficients in the Shendong mining area. J. Clean. Prod. 244, 118646.

Subba Rao, N., Dinakar, A., Surya Rao, P., Rao, P.N., Madhnure, P., Prasad, K.M., Sudarshan, G., 2016. Geochemical processes controlling fluoride-bearing groundwater in the granitic aquifer of a semi-arid region. J. Geol. Soc. India 88 (3), 350–356.

Tarki, M., Dassi, L., Hamed, Y., Jedoui, Y., 2011. Geochemical and isotopic composition of groundwater in the Complex Terminal aquifer in southwestern Tunisia, with emphasis on the mixing by vertical leakage. Environ. Earth. Sci. 64, 85–95.

Van Voast, W.A., 2003. Geochemical signature of formation waters associated with coalbed methane. AAPG Bull. 87 (4), 667–676.

Wallin, B., Peterman, Z., 2015. Compilation and review of 87Sr/86Sr and stable isotopes from groundwater, calcite fracture fillings, mineral, and whole-rock sampling at Äspö, Sweden. Groundwater 53 (s1), 103–112.

Wang, C.S., Sun, Y.J., Miao, X.X., Yang, G.Y., 2008. History of Water Conservation in Shendong Mining Area, China. 10th International-Mine-Water-Association Congress on Mine Water and the Environment, Karlovy Vary, Czech Republic. JUN 02-05.

Wang, G.X., Cheng, G.D., 2001. Fluoride distribution in water and the governing factors of environment in arid north-west China. J. Arid Environ. 49, 601–614.

Wang, L.H., Dong, Y.H., Xie, Y.Q., Song, F., Wei, Y.Q., Zhang, J.Y., 2016. Distinct groundwater recharge sources and geochemical evolution of two adjacent sub-basins in the lower Shule River Basin, northwest China. Hydrogeol. J. 24, 1967–1979.

Wang, Z.R., Tian, X., Wu, X., 2018. Hydrochemical characteristics and quality assessment of shallow groundwater and CBM co-produced water in the Shizhuangnan block, Qinshui Basin, China. Environ. Earth Sci. 77, 57.

Weinstein, L.H., Davison, A., 2004. Fluoride in the Environment: Effects on Plants and Animals. CABI Publishing, Wallingford, U.K.

Wen, D.G., Zhang, F.C., Zhang, E.Y., Wang, C., Han, S.B., Zheng, Y., 2013. Arsenic, fluoride and iodine in groundwater of China. J. Geochem. Explor. 135, 1–21.

Whiticar, M.J., 1999. Carbon and hydrogen isotope systematics of bacterial formation and oxidation of methane. Chem. Geol. 161, 291–314.

WHO, 1996. Total Dissolved Solids in Drinking-Water. Background Document for Development of WHO Guidelines for Drinking-water Quality, Geneva.

WHO, 2006. Fluoride in Drinking Water by J. Fawell, K. Bailey, J. Chilton, E. Dahi, L. Fewtrell and Y. Magara. (Published by). WA Publishing, London, UK, p. 134.

WHO, 2017. Guidelines for Drinking-Water Quality: Fourth Edition Incorporating the First Addendum (Fourth). World Health Organization.

Contemporary reviews of mine water studies in Europe, part 2. In: Wolkersdorfer, C., Bowell, R. (Eds.), Mine Water Environ. 24, 2–37.

Wu, L.J., 2001. The Deposit Environment Analysis of Shendong Mining Area and Research of the Influence on Coal Mining Geology Condition. Master thesis. Liaoning Technical University, Fuxin, China (in Chinese with English abstract).

Xu, J.M., Zhu, W.B., Xu, J.L., Wu, J.Y., Li, Y.C., 2021. High-intensity longwall mining-induced ground subsidence in Shendong coalfield, China. Int. J. Rock Mech. Min. 141, 104730.

Xue, J.H., Lee, C., Wakeham, S.G., Armstrong, R.A., 2011. Using principal components analysis (PCA) with cluster analysis to study the organic geochemistry of sinking particles in the ocean. Org. Geochem. 42, 356–367.

Yuan, J.F., Xu, F., Deng, G.S., Tang, Y.Q., Li, P.Y., 2017. Hydrogeochemistry of shallow groundwater in a Karst aquifer system of Bijie city, Guizhou province. Water 9, 625.

Zhang, Z., Qin, Y., 2018. A preliminary investigation on water quality of coalbed natural gas produced water for beneficial uses: a case study in the Southern Qinshui Basin, North China. Environ. Sci. Pollut. Res. 25 (22), 21589–21604.

Zhang, Z., Yan, D.T., Zhuang, X.G., Yang, S.G., Wang, G., Li, G.Q., Wang, X.M., 2019. Hydrogeochemistry signatures of produced waters associated with coalbed methane production in the Southern Junggar Basin, NW China. Environ. Sci. Pollut. Res. 26, 31956–31980.